THE JOURNAL OF PHYSICAL CHEMISTRY A

ARTICLE

pubs.acs.org/JPCA

# Kinetics and Solvent-Dependent Thermodynamics of Water Capture by a Fullerene-Based Hydrophobic Nanocavity

Michael Frunzi,[†] Anne M. Baldwin,[†] Nobuyuki Shibata,[‡] Sho-Ichi Iwamatsu,[‡] Ronald G. Lawler,[§] and Nicholas J. Turro[†,*]

[†]Department of Chemistry, Columbia University, New York, New York 10027, United States of America

[‡]Graduate School of Environmental Studies, Nagoya University, Chikusa-ku, Nagoya, Aichi 464-8601, Japan

[§]Department of Chemistry, Brown University, Providence, Rhode Island 02912-9108, United States of America

Supporting Information

**ABSTRACT:** Kinetic and thermodynamic properties of water encapsulation from organic solution by an open-cage [60]fullerene derivative have been investigated. 2D exchange NMR spectroscopy (EXSY) measurements were employed to determine the association and dissociation constants at 300−330 K ($k_a$ = 4.3 $M^{-1} \times s^{-1}$ and $k_d$ = 0.42 $s^{-1}$ at 300 K) in 1,1,2,2-tetrachloroethane-$d_2$ as well as the activation energies ($E_{a,ass}$ = 27 kJ $mol^{-1}$, $E_{a,diss}$ = 50 kJ $mol^{-1}$). The equilibrium constants and thermodynamic parameters in various solvents (benzene-$d_6$, 1,2-dichlorobenzene-$d_4$, and dimethylsulfoxide-$d_6$) were estimated using 1D-$^1$H NMR spectroscopy. The parameters were dependent on the polarity of the solvent; $\Delta H$ depended linearly on the solvent polarity, becoming increasingly unfavorable as polarity increased. Mixtures of polar dimethylsulfoxide-$d_6$ in less polar 1,1,2,2-tetrachloroethane-$d_2$ showed a similar trend.

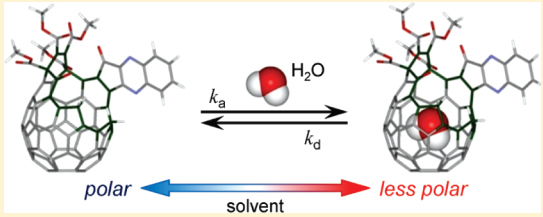


## INTRODUCTION

The topic of confinement of water in hydrophobic spaces may seem academic or perhaps counterintuitive, but it is a subject of increasing importance.[1,2] Additionally, molecular encapsulation has widespread applications in molecular recognition and catalysis, as well as protecting encapsulated molecules from degradation in their surrounding environment. Nonpolar or weakly polar pores capable of capturing water exist in many protein channels and proton pumps.[2−4] The escape of water from protein structures has significant implications for the kinetic stability and functionality of proteins, for instance, the motion of $H_2O$ out of hydrophobic spaces drives the type I $Ca^{2+}$ secretion switch.[5] Furthermore, it has been postulated that motions of fluids like water through porous nanostructures could be harnessed to generate clean electricity, employing the ambient mechanical motions and heat.[6−10] In these confined regimes, water behaves differently than in bulk phases. It is therefore of vital importance that the interactions between water and hydrophobic spaces be understood and characterized.

A wide variety of systems have been developed to trap small amounts of water molecule(s). Successful capsules include oligomer or polymer helices,[11] some cavitands,[12] and chemically opened fullerenes.[13−19] The last fullerenes are generally described as open-cage fullerenes.[20−23] The inner sphere of the most abundant fullerene, $C_{60}$, has been estimated to be approximately 3.5 Å in diameter,[20] similar to common desiccants, 3- or 4-Å molecular sieves. To access the closed interior of a fullerene, carbon−carbon bonds of the `cage' must be cleaved by organic reactions designed to afford either resealable or permanent openings. Openings of this size permit the insertion of noble gas atoms (He, Ne, Ar, and Kr) and small molecules ($H_2$, $N_2$, CO, $H_2O$, $NH_3$, and $CH_4$) inside the host.[20−26] Generally, high temperatures and pressures are employed for insertion, so that the guest remains inside once ambient conditions are returned. Fullerenes with larger openings, like compound **1** (Figure 1), have also been shown to spontaneously encapsulate a single $H_2O$ from organic solution.[13] This behavior is intriguing; the supposedly hydrophobic cage interior must be somehow stabilizing the $H_2O$, as the loss in entropy alone should preclude this. Exploration of this phenomenon could provide insight into dynamics of $H_2O$ into and out of confinement, the energetics of the process, and perhaps yield new ideas to drive and direct water in hydrophobic spaces.

Enthalpic forces should be driving the spontaneous $H_2O$ encapsulation by **1**. To date, however, only the following experimental evidence has been found: (1) A residual water molecule in a solvent is spontaneously encapsulated by **1**, without any additional force. (2) The fraction of $H_2O$@**1** to empty **1** is generally in the range of 50−75% in a solution, and it is dependent on the water content of a used solvent. (3) The trapped water molecule shows rapid exchange with another $H_2O$

**Received:** November 12, 2010
**Revised:** December 15, 2010
**Published:** January 10, 2011

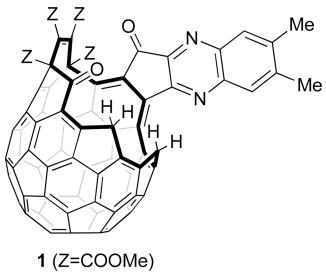


**1** (Z=COOMe)

**Figure 1.** Open-cage fullerene, **1**.

(or $D_2O$) in a solvent. (4) X-ray crystal structures have verified the presence of an $H_2O$ inside a similar cage.[23]

Herein, we report kinetic and thermodynamic properties of this process. The protons of water and functional groups in **1** make analyses possible using 1D $^1$H NMR and 2D $^1$H−$^1$H EXSY (EXchange SpectroscopY) spectroscopies; standard differential scanning calorimetry (DSC) can also be employed. The former have been widely employed for the kinetic and thermodynamic investigations in host−guest chemistry. The effect of various solvents on encapsulation will also be tested.

## METHODS

**Sample Preparation.** Compound **1** was synthesized according to the published methods.[13,20] Typically, 50−75% (depends on the solvent) of the dissolved **1** encapsulate one $H_2O$ molecule to form $H_2O$@**1** in a solution at ambient temperature. NMR solutions were prepared using 0.5−4 mg of the purified **1** per 500 $\mu$L of an NMR solvent, depending upon solubility of **1**. 1,1,2,2-tetrachloroethane-$d_2$ (TCE-$d_2$), 1,2-dichlorobenzene-$d_2$ (ODCB-$d_4$), benzene-$d_6$ ($C_6D_6$), and dimethylsulfoxide-$d_6$ (DMSO-$d_6$) were chosen as the solvents. A series of mixed solvents of TCE-$d_2$ and DMSO-$d_6$ were prepared with the following ratios; TCE-$d_2$ ($\mu$L): DMSO-$d_6$ ($\mu$L) = 475:25, 450:50, and 425:75. Each solution was placed in an NMR tube, evacuated to less than 1 Torr, and flame-sealed before measurements.

**2D $^1$H−$^1$H EXSY NMR Spectroscopy.** 2D $^1$H−$^1$H EXSY spectra[27,28] were taken of 1.0−6.0 mg of **1** in 500 $\mu$L of 1,1,2,2-tetrachloroethane at 300, 310, 320, and 330 K on a Bruker Avance III 400-MHz spectrometer. Mixing times of 2.50, 2.00, 1.80, and 1.25 s, respectively, were used. Typically, resolution of 2048 × 128 was selected, and 12 scans per point were taken. These were compared against reference spectra with minimal mixing times of 0.03 s. Magnetization exchange rate constants were then calculated using ExsyCalc software.[29]

**1D $^1$H NMR Spectroscopy.** The $^1$H NMR spectra were taken on a Bruker DRX 300-MHz spectrometer. All chemical shifts were relative to TMS. Line broadening optimized from unprocessed peak fwhm values (up to 3 Hz) was used to improve the signal-to-noise ratio. The experiments were taken at 4 temperatures, 300, 310, 320, and 330 K; the samples were allowed to equilibrate in the probe for at least 15 min before the spectra were taken. Line-fitting was carried out using MestraNova 6.0 software.

**Fluorescence Spectroscopy.** A 2 $\mu$M pyrene solution was prepared in TCE as a fluorescence probe of solvent polarity via serial dilution.[30] Emission of the probe molecule was recorded on a Horiba Jobin Yvon FluoroMax-2 Spectometer with an excitation wavelength of 350 nm scanning from 365 to 420 nm using a 0.5 s integration time.

**DSC Measurement.** Compound **1** (4.9−5.1 mg) was enclosed in an aluminum pan and placed in a TA Instruments Q100 differential scanning calorimeter.[14] All measurements were conducted under a nitrogen atmosphere (50 mL/min) using the cyclic cooling/heating program as follows: (1) Purge with nitrogen gas for 10 min at 35 °C, (2) cool the sample to −40 °C by 10 °C/min ramping and hold that temperature for 10 min, (3) heat to 200 °C by 10 °C/min ramping and hold that temperature for 10 min, (4) cool to −40 °C by 10 °C/min ramping and hold for 10 min, (5) heat to 200 °C by 10 °C/min ramping and hold for 10 min, and (6) cool to 35 °C by 10 °C/min ramping.

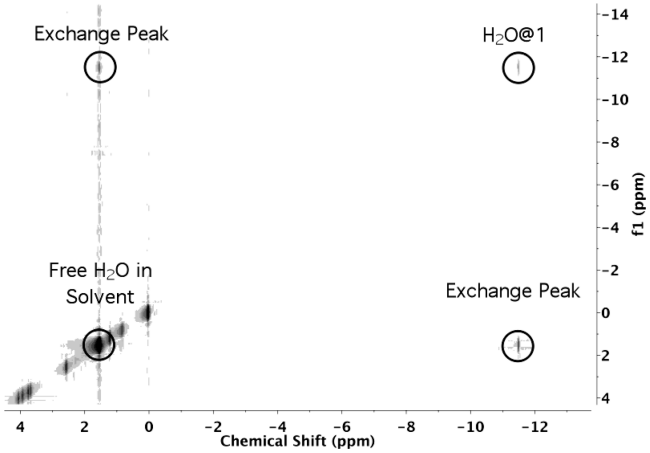


**Figure 2.** 2D $^1$H−$^1$H EXSY of the encapsulation of $H_2O$ by **1** in TCE-$d_2$ at 300 K.

## RESULTS AND DISCUSSION

**Exchange Behaviors of $H_2O$ Encapsulation and Escape from 1.** $^1$H−$^1$H 2D EXSY (NOESY) has been shown to measure the exchange of small organic guests into and out of cavitand−porphyrin hosts.[31] Here it was used to determine the rate constants for the release and encapsulation of $H_2O$ into **1** in TCE-$d_2$. The off-diagonal peaks in these spectra are proportional to the rates of chemical exchange between the two corresponding sites. Mixing times (the delay between the second and third pulses) were selected to allow maximal chemical exchange to occur while minimizing loss of the magnetization created by the first two pulses. The resultant spectra had only two cross-peaks, demonstrating clear exchange between the free water ($\delta$ = 1.6 ppm) and endohedral water resonance ($\delta$ = −11.5 ppm). A sample EXSY spectrum is given in Figure 2.

Perrin and Dwyer describe a method to interpret absolute kinetic rates from EXSY observed rates.[27] Equations 1−3 give a simple treatment of the equilibrium where [H], [G], and [G@H] are the concentrations of the free host, free guest, and the complex, respectively, and $k'_1$ and $k'_{-1}$ are the "observed" rates found from the areas of the two EXSY spectrum exchange peaks.[31]

$$\frac{d[\mathrm{G@H}]}{dt} = k_a[\mathrm{H}][\mathrm{G}] - k_d[\mathrm{G@H}] \quad (1)$$

$$[\mathrm{G}] \underset{k'_{-1}}{\overset{k'_1}{\leftrightarrow}} [\mathrm{G@H}] \quad (2)$$

$$k'_1 \approx k_a[H] \quad k'_{-1} \approx k_d \quad (3)$$

Concentration of free host was calculated from the mass of **1** and the volume of solvent added to the NMR tube. From the 1D NMR, the percentage of "filled" fullerene was found by dividing


dx.doi.org/10.1021/jp110832m |J. Phys. Chem. A 2011, 115, 735–740

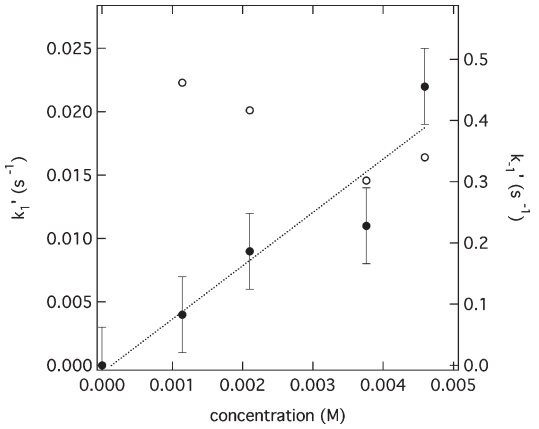


**Figure 3.** Observed rate constants, $k'_1$ (filled circle, left axis) and $k'_{-1}$ (open circle, right axis), vs concentration of the unbound host **1** in TCE-$d_2$ at 300 K from 2D $^1$H−$^1$H EXSY.

**Table 1. Association Rate, Dissociation Rate, and Equilibrium Constants of $H_2O$@1 in TCE-$d_2$ Determined from 2D EXSY**

| temperature (K) | $k_a$ ($M^{-1} \times s^{-1}$) | $k_d$ ($s^{-1}$) | $K_{eq}$ ($M^{-1}$) |
|---|---|---|---|
| 300 | 4.3 | 0.42 | 10 |
| 310 | 5.8 | 1.1 | 5.3 |
| 320 | 8.3 | 1.7 | 4.9 |
| 330 | 11.2 | 2.7 | 4.1 |

the area of the $H_2O$@**1** resonance by a signal from two external protons on the host. With the concentration of guest@host and total host, empty [H] was found via simple subtraction.

It was verified that the kinetics obey eq 3 by determining the rate constants at various concentrations of **1** at 300 K. Indeed, $k'_1$ displayed a linear dependence on concentration of **1** with a slope of 4.2 $M^{-1} \times s^{-1}$. Conversely, $k'_{-1}$ changed little with respect to the amount of **1** in solution, approximately 20% from the mean value, similar to a methane- and ethylene-encapsulating cavitand.[31] Plots of the observed EXSY rates vs concentration of **1** are given in Figure 3.

The rate constants ($k_a$ and $k_d$) were obtained at four different temperatures (300−330 K) by the 2D $^1$H−$^1$H EXSY experiments.[27,31] The results are given in Table 1, and the Arrhenius plot of $k_a$ is shown in Figure 4. Further, thermodynamic parameters derived from them are summarized in Table 2. As shown in Table 1, the observed rates clearly indicate that the association of water and hydrophobic cavity **1** is a favored process, as expected. Relatively low activation energies ($E_a$) for both association and dissociation support the observed rapid exchange behavior of $H_2O$ as well as related parameters for the transition state. The large $\Delta S^{\ddagger}$ for both association and dissociation of $H_2O$ into **1** also indicate that the guest is severely restricted in the transition state, passing through the narrow orifice. Correspondingly, the orifice seems to provide little enthalpic stabilization leading to large values of $\Delta G^{\ddagger}$ for the encapsulation and escape reactions.

It was found that the observed rates for both the $H_2O$ encapsulation and escape were much faster ($10^4\times$) than those observed for the CO escape from CO@**1**.[16] The fraction of CO@**1** was low (less than 20%) under a balloon pressure of

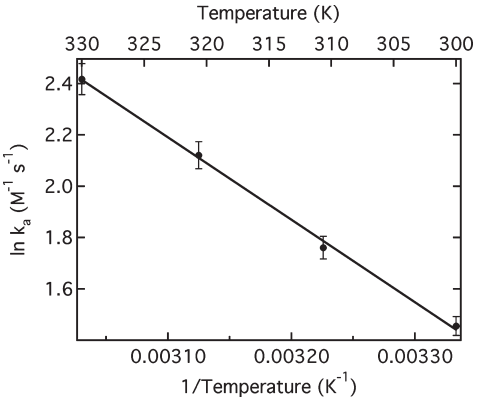


**Figure 4.** Arrhenius plot of the encapsulation of $H_2O$ by **1**.

**Table 2. Thermodynamic Parameters in TCE-$d_2$ Determined from 2D EXSY Rate Constants**

| | | | |
|---|---|---|---|
| $\Delta G°$ (kJ/mol)[a] | −5.2 | $\Delta G^{\ddagger}_{ass}$ (kJ/mol)[f] | 70 |
| $\Delta H°$ (kJ/mol)[b] | −24 | $\Delta G^{\ddagger}_{diss}$ (kJ/mol)[f] | 76 |
| $\Delta S°$ (J/mol × K)[c] | −63 | $\Delta H^{\ddagger}_{ass}$ (kJ/mol)[g] | 24 |
| $E_{a,ass}$ (kJ/mol)[d] | 27 ± 2 | $\Delta H^{\ddagger}_{diss}$ (kJ/mol)[g] | 48 |
| $E_{a,diss}$ (kJ/mol)[e] | 50 ± 6 | $\Delta S^{\ddagger}_{ass}$ (J/mol × K)[h] | −167 |
| $\ln(A)_{ass}$ ($M^{-1} \times s^{-1}$)[d] | 12 ± 1 | $\Delta S^{\ddagger}_{diss}$ (J/mol × K)[h] | −93 |
| $\ln(A)_{diss}$ ($s^{-1}$)[e] | 19 ± 2 | | |

[a] $\Delta G° = RT \ln K_{eq}$. [b] $\Delta H° = E_{a,ass} - E_{a,diss}$. [c] $\Delta G° = \Delta H° - T\Delta S°$. [d] From Arrhenius plot of $k_a$. [e] From Arrhenius plot of $k_d$. [f] From the Eyring equation. [g] From the Eyring plot. [h] $\Delta S^{\ddagger} = -(\Delta G^{\ddagger} - \Delta H^{\ddagger})/T$.

CO,[15] while $H_2O$ spontaneously enters in **1** at 300 K.[13] Significant CO encapsulation into **1** requires high pressures and temperatures (80−100 atm at 373 K). This disparity is not surprising since $H_2O$ is much smaller than CO; respective van der Waal's radii are 1.443 and 2.276 Å.[32] The pre-exponential factor for the escape is also smaller for $H_2O$ than for CO leaving **1**,[17] indicating more collisions between the host and the larger CO guest inside; however, the large difference in $E_a$ for the CO and $H_2O$ escape accounts for the disparity in behaviors.

While the observed $H_2O$ exchange was too fast to observe with standard 1D $^1$H NMR, it was 2 orders of magnitude slower than the rates of $CH_4$ encapsulations by cavitands and cryptophanes.[31,33,34] Compared with these systems ($K_{eq} \approx 230\ M^{-1}$), smaller $K_{eq}$ (~10 $M^{-1}$) were obtained for the formation of $H_2O$@**1** from the EXSY rate constants. Determination of equilibrium constants via 1D NMR and Karl Fisher titration is discussed later.

The thermodynamics properties of this reaction resemble those for both cavitand porphyrins that spontaneously encapsulate dissolved $CH_4$[31,33] as well as hydrogen-bonding cavitands that bind water from organic solution at low temperatures (−50 °C).[12] However, in both cases the change in free energy is lower for the formation of $H_2O$@**1**, possibly due to the polar nature of $H_2O$. In the former comparison, the guest and host were both hydrophobic, and in the latter, hydrogen bonding stabilizes the polar guest. $H_2O$@**1** is unique in that the polar guest is likely bound by dispersive interactions only. Despite this, the encapsulation is exothermic even at elevated temperatures. One final note is that the loss in entropy for $H_2O$ entering **1** is


dx.doi.org/10.1021/jp110832m |J. Phys. Chem. A 2011, 115, 735–740

**Table 3. Thermodynamic Parameters of $H_2O$@1 Formation in Various Solvents determined from 1D NMR**

| solvent | dipole moment (D) | $\Delta H°$ (kJ/mol) | $\Delta S°$ (J/mol × K) |
|---|---|---|---|
| benzene-$d_6$ | 0 | $-35 \pm 5$ | $-92 \pm 15$ |
| TCE-$d_2$[a] | 1.2 | $-25 \pm 4$ | $-72 \pm 10$ |
| ODCB-$d_4$[b] | 2.4 | $-18 \pm 1$ | $-33 \pm 4$ |
| DMSO-$d_6$[c] | 3.9 | N/A[d] | N/A[d] |

[a] 1,1,2,2-Tetrachloroethane-$d_2$. [b] 1,2-Dichlorobenzene-$d_4$. [c] Dimethylsulfoxide-$d_6$. [d] $H_2O$ does not enter **1** in DMSO-$d_6$.

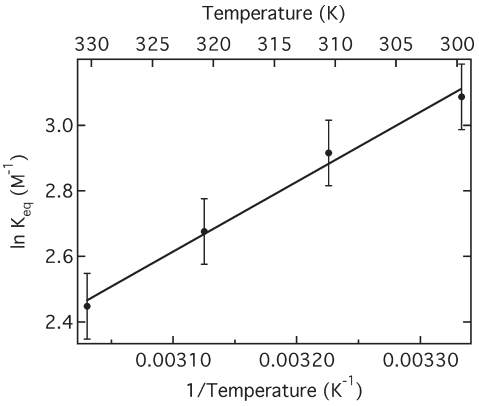


**Figure 5.** Van't Hoff plot of the $H_2O$ + **1** ⇆ $H_2O$@**1** equilibrium in ODCB-$d_4$.

much less compared to the hydrogen-bonding cavitand, perhaps because the guest is freer to move around in **1**.

**Encapsulation and Escape Thermodynamics in Pure Solvents and Mixtures.** The key to understanding and eventually controlling the encapsulation of water may lie in changes to the exterior as much as the interior of the host. When a water molecule is trapped in **1**, the fullerene must be providing more stabilization than the solvent system. We therefore treated the solvent used for **1** as a tunable exterior instead of a barely tunable interior, the cage **1**. Modulating the solvent parameters was expected to show some effects on the equilibrium and kinetics. It is worthy to note that, because of limited solubility of fullerenes, solvents chosen for a fullerene derivative are generally hydrophobic as well as the interior of a fullerene cage.[24−26]

The equilibrium concentrations of $H_2O$@**1**, **1**, and $H_2O$ in different organic solvents ($C_6D_6$, TCE-$d_2$, ODCB-$d_4$, and DMSO-$d_6$) were estimated via the $^1$H NMR measurements at various temperatures. The relative amounts of the total **1**, $H_2O$@**1**, and free $H_2O$ were calculated from the signals at $\delta$ = 8.1 ppm (aromatic protons characteristic of both **1** and $H_2O$@**1**), 1.6 ppm (free $H_2O$ in a solvent), and −11.5 ppm ($H_2O$ trapped in $H_2O$@**1**), respectively.[13] These were converted to concentrations and used to find $K_{eq}$ at each temperature. Thermodynamic parameters can be interpolated from the slope and intercept of a Van't Hoff plot ($\ln K_{eq}$ vs $1/T$). These results are summarized in Table 3. Additionally, as exemplar, the Van't Hoff plot of the $H_2O$@**1** formation in ODCB-$d_4$ is given in Figure 5.

A significant solvent effect was observed as shown in Table 3. Both $\Delta H$ and $\Delta S$ decreased in less polar $C_6D_6$ and increased in more polar ODCB-$d_4$. The loss of entropy when a $H_2O$ molecule "leaves" bulk benzene to enter **1** is comparatively large, while the observed loss in entropy is far smaller in case of the ODCB-$d_4$ solutions; the $H_2O$ molecules in ODCB-$d_4$ may be slightly ordered by polar interactions, so less disorder is effectively lost. The large loss of entropy upon insertion must be offset by enthalpic gains. Moreover, $H_2O$ did not enter the host **1** in highly polar DMSO-$d_6$ at room temperature. Clearly, less polar solvents drive the water encapsulation by **1**, and the observed changes in thermodynamic parameters appear almost linear compared to the polarity of the solvents. Essentially, stabilization by a used solvent is competing with that by the host **1**.

The thermodynamic parameters parameters given in Table 3 were found for the encapsulation of $H_2O$ into **1** were found from line-fitting the 1D $^1$H NMR spectra. Compared to the values found in 2D EXSY measurements (Table 2), the TCE-$d_2$ data for $\Delta H$ is in very close agreement, while $\Delta S$ is 15% larger. Typically, the $K_{eq}$ values are slightly larger in the 1D fits, ranging from 10 to 30 $M^{-1}$ at 300 K, depending on solvent. Nakazawa et al. reported a much larger disparity between $K_{eq}$ values derived from EXSY and 1D methods, 230 and 80 $M^{-1}$, respectively.[31] Major sources of error here are likely from uncertainty in the line fits and integration of the 1D and 2D spectra, respectively, especially in the large free $H_2O$ peaks. While [$H_2O$] in the organic solvent is not greatly affected by the reaction ([$H_2O$] is at least 5× greater than [**1**], and the amount of $H_2O$ inside **1** changes by <25%), the amount of free $H_2O$ in the organic solvents is also affected by changes in solubility of $H_2O$ across the temperature range, the vapor pressure of $H_2O$ in the tube, etc. Additionally, the low signal-to-noise ratio of the $H_2O$@**1** signal at high temperatures increases error. Karl Fisher titration was attempted to better determine more accurate [$H_2O$] values for the encapsulation in $CDCl_3$. Equilibrium constants were somewhat higher using this method (~45 $M^{-1}$), but $\Delta H$ was in relatively good agreement for a solvent similar to TCE-$d_2$. This titration experiment is detailed in the Supporting Information.

The solubility of compound **1** initially limited the extent to which this effect could be explored, so mixtures of TCE-$d_2$ and DMSO-$d_6$ were prepared. Again, equilibrium constants were determined from 1D $^1$H NMR spectra as above. The polarity of the solvent mixture should increase as DMSO-$d_6$ is added to the solution. The relative polarities of the mixtures were determined using fluorimetry.[30] The vibrational fine structure of the pyrene monomer fluorescence depends on the dipole moment of its bulk solvent. The ratio of the intensities of the 0−0 (peak I) and 0−2 (peak III) fluorescence bands of pyrene in the different solvent mixtures indicates their relative polarities. This procedure is described in detail by Kalyanasundaram et al.[30] A dilute pyrene solution was prepared in the following TCE-$d_2$:DMSO-$d_6$ mixtures to determine their relative polarity. Compound **1** was then dissolved in these and the 1D NMR measurement was repeated. The thermodynamic data are given in Table 4.

As shown in Table 4, the trend seen in the pure solvents is repeated here. Apparently, $H_2O$ can be "driven out of" the cage by spiking a solvent with a very polar solvent. While it was impossible to determine the rate rigorously, $H_2O$@**1** initially in 500 $\mu$L pure TCE-$d_2$ established a new equilibrium (50% encapsulation reducing to 25%) after the addition of 50 $\mu$L DMSO-$d_6$, in no more than 30 s (this was the amount of time it took to add the additional solvent and take an $^1$H NMR scan).

**Binding Energy between the Trapped $H_2O$ and the Fullerene Cage 1.** Since the discovery of endohedral fullerene complexes, binding energies between the host fullerenes and the trapped guests inside have been investigated mainly in theory.[35,36] For $H_2O$@$C_{60}$, binding energy ($\Delta E$) of a $H_2O$

**Table 4. Thermodynamic Parameters of $H_2O$@1 Formation in Solvent Mixtures of TCE-$d_2$ and DMSO-$d_6$ Determined from 1D NMR**

| (TCE:DMSO) | ratio peak III/peak I | $\Delta H°$ (kJ/mol) |
|---|---|---|
| (100:0) | 0.702 | $-25 \pm 4$ |
| (95:5) | 0.686 | $-20 \pm 4$ |
| (90:10) | 0.681 | $-16 \pm 3$ |
| (88:12) | 0.679 | $-13 \pm 3$ |

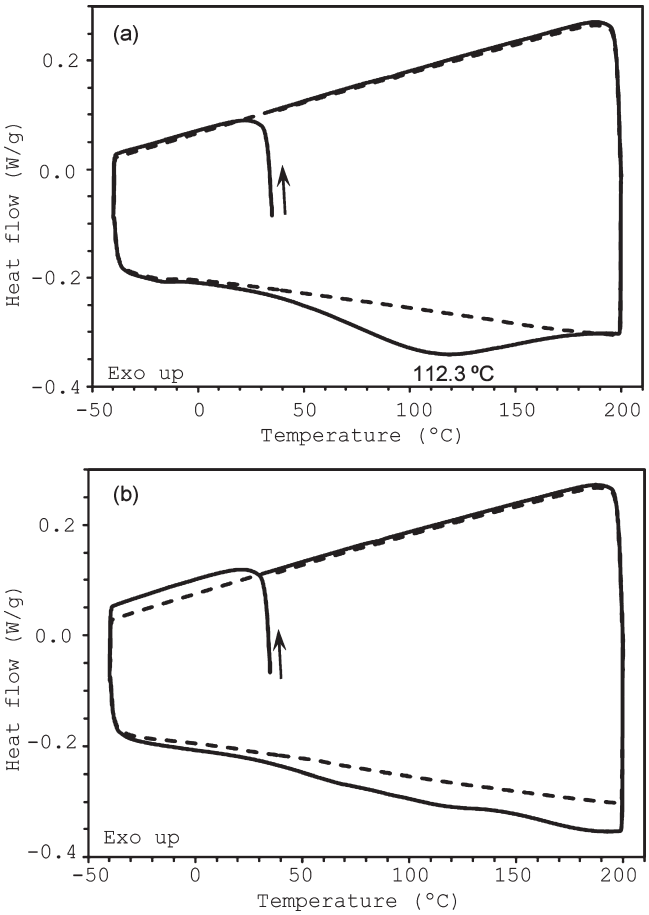


**Figure 6.** DSC charts of (a) $H_2O$@**1** and (b) CO@**1** as reference. The initial and second cycles are shown as plain and dotted lines, respectively (ramp 10 °C/min, hold temperature for 10 min at −40 °C and at 200 °C).

molecule inside the $C_{60}$ cage was estimated to be −44 kJ $mol^{-1}$ at the MP2/6-31G level; however, it is unclear how basis set superposition error (BSSE) was accounted for.[37−39] Since computationally intensive thermochemical data are needed to find $\Delta H$, reliable calculations are rare.

The mild conditions of this encapsulation provide a rare opportunity to estimate an absolute $\Delta H$ of encapsulation for a fullerene from actual experiment. Our data for the change of enthalpy for the encapsulation of $H_2O$ in benzene allows for an estimate of the total $\Delta H$ for the insertion of $H_2O$. Nilsson reported that the $\Delta H_{solvation}$ of $H_2O$ into benzene is 24 kJ/mol;[40] therefore, by assumption of a state function, the total enthalpic stabilization of vapor-phase $H_2O$ into **1** is approximately −11 kJ/mol.

A thermal analysis of $H_2O$@**1** using DSC was attempted.[14] A DSC trace of solid-state $H_2O$ escape from **1** is shown in Figure 6a. A broad endothermic curve was observed with a maximum temperature at 112 °C in the first heating process. It showed a good agreement with the temperature range for an escape of $H_2O$ from $H_2O$@**1** in a solution monitored by $^1H$ NMR.[13] The same endothermic curve was not observed in the second heating process. In addition, a reference CO@**1** did not show significant peak such as $H_2O$@**1** (Figure 6b). Note that detectable drift during the first heating of CO@**1** was caused by contaminate $H_2O$@**1** (ca. 5% by $^1H$ NMR), which made a precise measurement of CO@**1** impossible. The observed endothermic curve was therefore concluded to correspond to the solid-state thermal escape of $H_2O$ from $H_2O$@**1**. The binding energy of a trapped $H_2O$ molecule was estimated to be approximately −58 kJ $mol^{-1}$. This assumes the initial fraction of $H_2O$@**1** in the solid **1** as 75% from elemental analysis. However, elemental analysis is unable to differentiate endohedral water from water elsewhere in the sample (for instance, impurities and interstitial spaces). This value seems suspiciously large; perhaps additional energy is required to liberate the $H_2O$ from the solid lattice once it exits the fullerene.

## CONCLUSIONS

The kinetic and thermodynamic properties for the encapsulation of $H_2O$ by compound **1** in various organic solvents were determined. The rates at 300 K were 4.3 $M^{-1} \times s^{-1}$ for encapsulation and 0.42 $s^{-1}$ for escape, far faster than for larger guests in this host. The activation energies were 27 and 50 kJ $mol^{-1}$ for association and dissociation, respectively. The change in enthalpy for the encapsulation is linearly dependent on the polarity of the solvent system and both pure solvents and solvent mixtures were explored. By use of the values found for encapsulation in benzene, the absolute $\Delta H$ for the encapsulation of $H_2O$ by **1** was estimated by solution-state NMR to be −11 kJ $mol^{-1}$ and in solid-state NMR −58 kJ $mol^{-1}$ by DSC. The swift water transfer controlled by the polarity of the external solvent media could be useful for future applications that require $H_2O$ to move into and through hydrophobic spaces like nanotubes as well as water-induced conformational changes in proteins.

## ASSOCIATED CONTENT

**Supporting Information.** Data related initial NMR study combined with Karl Fischer titrations. This material is available free of charge via the Internet at http://pubs.acs.org.

## AUTHOR INFORMATION

**Corresponding Author**
*E-mail: njt3@columbia.edu.

## ACKNOWLEDGMENT

We thank the National Science Foundation for its continued and generous support of this research through Grant CHE 07-17518 as well as the NSF REU program. A part of this work was supported by Grant-in-Aid for Scientific Research (C) (No.20550122) from Japan Society for the Promotion of Science. Research Center of Computer Science at the Institute for Molecular Science is also acknowledged for the computational resource.

## REFERENCES


(1) Rasaiah, J. C.; Garde, S.; Hummer, G. *Annu. Rev. Phys. Chem.* **2008**, *59*, 713.
(2) Matthews, B. W.; Liu, L. J. *Protein Sci.* **2009**, *18*, 494.
(3) Eriksson, A. E.; Baase, W. A.; Zhang, X. J.; Heinz, D. W.; Blaber, M.; Baldwin, E. P.; Matthews, B. W. *Science* **1992**, *255*, 178.
(4) Ernst, J. A.; Clubb, R. T.; Zhou, H. X.; Gronenborn, A. M.; Clore, G. M. *Science* **1995**, *267*, 1813.
(5) Blenner, M. A.; Shur, O.; Szilvay, G. R.; Cropek, D. M.; Banta, S. *J. Mol. Biol.* **2010**, *400*, 244.
(6) Hummer, G.; Rasaiah, J. C.; Noworyta, J. P. *Nature* **2001**, *414*, 188.
(7) Majumder, M.; Chopra, N.; Andrews, R.; Hinds, B. J. *Nature* **2005**, *438*, 930.
(8) Maniwa, Y.; Matsuda, K.; Kyakuno, H.; Ogasawara, S.; Hibi, T.; Kadowaki, H.; Suzuki, S.; Achiba, Y.; Kataura, H. *Nat. Mater.* **2007**, *6*, 135.
(9) Alexiadis, A.; Kassinos, S. *Chem. Rev.* **2008**, *108*, 5014.
(10) Liu, L.; Zhao, J. B.; Yin, C. Y.; Culligan, P. J.; Chen, X. *Phys. Chem. Chem. Phys.* **2009**, *11*, 6520.
(11) Garric, J.; Leger, J. M.; Huc, I. *Chem.—Eur. J.* **2007**, *13*, 8454.
(12) Ihm, C.; In, Y.; Park, Y.; Paek, K. *Org. Lett.* **2004**, *6*, 369.
(13) Iwamatsu, S.; Uozaki, T.; Kobayashi, K.; Re, S. Y.; Nagase, S.; Murata, S. *J. Am. Chem. Soc.* **2004**, *126*, 2668.
(14) Iwamatsu, S.; Murata, S.; Andoh, Y.; Minoura, M.; Kobayashi, K.; Mizorogi, N.; Nagase, S. *J. Org. Chem.* **2005**, *70*, 4820.
(15) Iwamatsu, S.; Stanisky, C. M.; Cross, R. J.; Saunders, M.; Mizorogi, N.; Nagase, S.; Murata, S. *Angew. Chem., Int. Ed.* **2006**, *45*, 5337.
(16) Stanisky, C. M.; Cross, R. J.; Saunders, M. *J. Am. Chem. Soc.* **2009**, *131*, 3392.
(17) Whitener, K. E.; Cross, R. J.; Saunders, M.; Iwamatsu, S.; Murata, S.; Mizorogi, N.; Nagase, S. *J. Am. Chem. Soc.* **2009**, *131*, 6338.
(18) Xiao, Z.; Yao, J. Y.; Yang, D. Z.; Wang, F. D.; Huang, S. H.; Gan, L. B.; Jia, Z. S.; Jiang, Z. P.; Yang, X. B.; Zheng, B.; Yuan, G.; Zhang, S. W.; Wang, Z. M. *J. Am. Chem. Soc.* **2007**, *129*, 16149.
(19) Pankewitz, T.; Klopper, W. *Chem. Phys. Lett.* **2008**, *465*, 48.
(20) Iwamatsu, S.; Murata, S. *Synlett* **2005**, 2117.
(21) Murata, M.; Murata, Y.; Komatsu, K. *Chem. Commun.* **2008**, 6083.
(22) Vougioukalakis, G. C.; Roubelakis, M. M.; Orfanopoulos, M. *Chem. Soc. Rev.* **2010**, *39*, 817.
(23) Gan, L. B.; Yang, D. Z.; Zhang, Q. Y.; Huang, H. *Adv. Mater.* **2010**, *22*, 1498.
(24) Hirsch, A.; Brettreich, M. Cluster Modified Fullerenes. In *Fullerenes: Chemistry and Reactions*; Wiley-VCH: Weinheim, 2005; pp 345.
(25) Iwamatsu, S.-i. Endohedral Fullerenes with Neutral Atoms and Molecule. In *Strained Hydrocarbons: Beyond the Van't Hoff and Le Bel Hypothesis*; Dodziuk, H., Ed.; Wiley-VCH: Weinheim, 2009; pp 282.
(26) Kitagawa, T. M., Y.; Komatsu, K. Fullerene Reactivity — Fullerene Cations and Open-Cage Fullerenes. In *Carbon-Rich Compounds: From Molecules to Materials*; Haley, M. M., Tykwinski, R. R., Eds.; Wiley-VCH: Weinheim, 2006; pp 383.
(27) Perrin, C. L.; Dwyer, T. J. *Chem. Rev.* **1990**, *90*, 935.
(28) Pastor, A.; Martnez-Viviente, E. *Coord. Chem. Rev.* **2008**, *252*, 2314.
(29) EXSYCalc is available at http://mestrelab.com/software/exsycalc/.
(30) Kalyanasundaram, K.; Thomas, J. K. *J. Am. Chem. Soc.* **1977**, *99*, 2039.
(31) Nakazawa, J.; Sakae, Y.; Aida, M.; Naruta, Y. *J. Org. Chem.* **2007**, *72*, 9448.
(32) Loeb, L. B. *Philos. Mag.* **1928**, *5*, 1011.
(33) Garel, L.; Dutasta, J. P.; Collet, A. *Angew. Chem., Int. Ed. Engl.* **1993**, *32*, 1169.
(34) Brotin, T.; Dutasta, J.-P. *Chem. Rev.* **2008**, *109*, 88.
(35) Cioslowski, J. *J. Am. Chem. Soc.* **1991**, *113*, 4139.
(36) Williams, C. I.; Whitehead, M. A.; Pang, L. *J. Phys. Chem.* **1993**, *97*, 11652.
(37) Ramachandran, C. N.; Sathyamurthy, N. *Chem. Phys. Lett.* **2005**, *410*, 348.
(38) Shameema, O.; Ramachandran, C. N.; Sathyamurthy, N. *J. Phys. Chem. A* **2005**, *110*, 2.
(39) Wang, L.; Zhao, J. J.; Fang, H. P. *J. Phys. Chem. C* **2008**, *112*, 11779.
(40) Nilsson, S. O. *J. Chem. Thermodyn.* **1986**, *18*, 877.